Hindawi
Journal of Nanotechnology
Volume 2023, Article ID 9940845, 10 pages
https://doi.org/10.1155/2023/9940845

Research Article

Unlocking the Potential of $NiSO_4 \cdot 6H_2O$/NaOCl/NaOH Catalytic System: Insights into Nickel Peroxide as an Intermediate for Benzonitrile Synthesis in Water

Abdel Ghany F. Shoair,[1] Abdulraheem S. A. Almalki,[2] Mai M. A. H. Shanab,[3] Ahmed M. Sheta,[4] Amir El-Basiony,[5] Nasser A. El-Ghamaz,[6] Hany A. Nasef,[7] and Hussein A. Khalaf[8]

[1]*Department of Science and Technology, University College-Ranyah, High Altitude Research Center, Prince Sultan Medical Complex Taif University, Taif 21975, Saudi Arabia*
[2]*Department of Chemistry, Faculty of Science, Taif University, Taif 21974, Saudi Arabia*
[3]*Department of Chemistry, College of Sciences and Humanities Studies (Girls Section), Hawtat Bani Tamim, Prince Sattam Bin Abdulaziz University, Al-Kharj 11149, Saudi Arabia*
[4]*Chemistry Department, Faculty of Science, Damietta University, New Damietta 34517, Egypt*
[5]*College of Nursing and Health Sciences, Al-Rayan Colleges AL-Madina Al-Munowara, Madina Almonawara 41411, P.O. Box 157, Saudi Arabia*
[6]*Department of Physics, Faculty of Science, Damietta University, New Damietta 34517, Egypt*
[7]*Department of Basic Science, Delta Higher Institute for Engineering and Technology, Mansoura 35681, Egypt*
[8]*Chemistry Department, Faculty of Science, Damanhour University, Damanhour, Egypt*

Correspondence should be addressed to Abdel Ghany F. Shoair; afshaair@tu.edu.sa

Received 7 September 2023; Revised 28 October 2023; Accepted 9 November 2023; Published 18 November 2023

Academic Editor: Samuel Lalthazuala Rokhum

Copyright © 2023 Abdel Ghany F. Shoair et al. This is an open access article distributed under the Creative Commons Attribution License, which permits unrestricted use, distribution, and reproduction in any medium, provided the original work is properly cited.

Nickel peroxide nanoparticles (NPNPs) were prepared and characterized using various techniques including transmission electron microscope (TEM), scan electron microscope (SEM), energy dispersive spectrometer (EDS), X-ray diffraction (XRD), and FTIR spectra. The aqueous basic catalytic system $NiSO_4 \cdot 6H_2O$/NaOCl/NaOH (pH = 14) was investigated for the catalytic dehydrogenation of benzylamine and parasubstituents to their corresponding nitriles at room temperature. The obtained results confirmed the formation of NiO_2 nanocrystalline particles with a size of 20 nm. Benzylamine with electron-donating groups showed higher yields of nitriles compared to electron-withdrawing groups. The mechanism involved in the in situ generated NiO_2 nanoparticles dehydrogenating benzylamine to benzonitrile, with the produced NiO converting back to NiO_2 nanoparticles through the excess of NaOCl.

1. Introduction

The green synthesis of organic compounds is of great importance for the protection of the environment from the dangerous climate changes [1]. Nitriles are very important functional group because of its presence in many pharmaceutical materials [2, 3]. Many drugs contain nitrile groups in their structures. Nitriles can enhance the biological activity of drugs by improving their stability, lipophilicity, and metabolic properties. For example, nitrile-containing drugs are used to treat hypertension, cancer, and diabetes [4]. Different strategies have been developed for the synthesis of nitriles such as the Sandmeyer reaction [5], Rosenmund-von Braun reaction [6], dehydration of amides and aldoximes [7], nucleophilic substitution of alkyl and aryl halides [8], and oxidation of amines [9]. However, these

methods often involve toxic reagents, harsh conditions, and produce chemical waste. Therefore, there is a strong need for an ecofriendly protocol. A number of transition metals such as ruthenium [10, 11], copper [12, 13], and nickel [14, 15] have been used for the catalytic hydrogenation of benzylamine to nitrile. Griffith and coworkers reported the catalytic dehydrogenation of benzyl amine by trans-$[RuO_3(OH)_2]^{2-}/S_2O_8^{2-}$ in aqueous alkaline medium [10]. Taube and coworkers reported the catalytic dehydrogenation of coordinated benzylamine to coordinated benzonitrile [11]. The simple copper-salt catalyst was used in the selective aerobic oxidation of amines to nitriles [12]. A number of aliphatic and aromatic amines were oxidized to nitriles by the $CuCl_2/O_2$ catalytic system in toluene as a solvent and at 80°C [13]. Nickel peroxide was used for the oxidation of many organic compounds [14]. Some alkylamines were dehydrogenated to their corresponding nitriles by $NiSO_4/K_2S_2O_8$ in good yields [15]. Pd@CuO, used as an anodic electrode, resulted in the electro-oxidative coupling of benzyl alcohol and ammonia, producing 83.2% of benzonitrile. This method was also successful in converting various primary alcohols to nitriles [16]. Xiao et al. [17] developed an efficient chemoenzymatic strategy to prepare nitriles from benzylamine by combining selective oxidation and dehydration.

Metal nanoparticles are of great interest to researchers due to their ease of synthesis, unique functional groups, and exceptional properties. They are significantly smaller than conventional materials and exhibit enhanced catalytic activity and increased thermal stability [18–21]. Several methods are used for metal nanoparticles preparation, e.g., sol-gel, hydrothermal, chemical vapor deposition, laser vaporization, plane pyrolysis, precipitation, and biosynthesis [21–23].

Nickel peroxide (NiO_2) nanoparticles have been investigated for their potential use in various applications, including catalysis, energy storage, and biomedical applications. They exhibit high stability, high thermal conductivity, and excellent electrochemical properties [24]. The synthesis of nickel oxide nanoparticles can be achieved using various methods, including sol-gel, hydrothermal, and thermal decomposition techniques [25, 26]. Sodium hypochlorite (bleaching house) is cheap, available, and environmentally acceptable chemical [27]. The synthetic applications of NaOCl in organic synthesis have been reported as a part of researchers' interest in the use of transition metals as a catalysts in organic synthesis [28–31]. NiO_2 serves as both a stoichiometric oxidant and a catalyst for the oxidation of benzyl alcohol. This implies that simultaneous stoichiometric and catalytic reactions can potentially take place in different reactions [31, 32].

According to Ji et al. [32], nanosized NiO_2 powder can be readily obtained by oxidizing Ni(II) salt with a hypochlorite solution, followed by a wet chemical method and calcination.

In this study, NiO_2 nanoparticles will be prepared at room temperature without using any capping agent compared to recently reported [26, 33, 34]. In addition, the optimum conditions and the mechanism of the catalytic dehydrogenation of benzylamine and some parasubstituents to their corresponding nitriles by the catalytic system, $NiSO_4{\cdot}6H_2O$/NaOCl, in an aqueous basic medium were investigated. Furthermore, the emphasis is placed on investigating several factors to optimize the reaction conditions.

2. Materials and Methods

2.1. Materials. $NiSO_4{\cdot}6H_2O$, benzylamine ($BzNH_2$), and p-substituted benzylamine R-$BzNH_2$ (R = CH_3, OCH_3, OH, NH_2, CHO, CN, NO_2, and F_3C) were used without purification and purchased from Sigma-Aldrich (Germany, Berlin) and NaOCl from local market.

2.2. NiO_2 Nanoparticles Preparation. NiO_2 nanoparticles were synthesized following a procedure described in the literature [31] but with a substitution of NaOCl and NaOH with K_2S_2O8 and KOH. In a typical method, 10 mL of 1.0 M NaOH was added to a solution containing $NiSO_4{\cdot}6H_2O$ (0.052 g, 0.2 mM) in 5 mL of H_2O. Subsequently, commercial NaOCl (10 mL, 14 mM, 5.25%, 0.7 M) was added dropwise with stirring, resulting in the formation of fine black particles. The precipitate was then filtered, washed with distilled water to remove NaCl, air-dried, and finally packed:

$$NiSO_4.6H_2O + NaOCl + 2NaOH \longrightarrow NiO_2 + NaCl + Na_2SO_4 + 7H_2O \quad (1)$$

2.3. Characterization. The phase identification (X-ray diffraction) was characterized using a JSX-60PA/Jeol diffractometer (Japan) equipped with a Ni-filtered CuKα radiation ($\lambda = 1.5418$ Å). Transmission electron microscopy (TEM) was carried out by using a JEM 100 CXII transmission electron microscope operating at 80 kV. The scanning electron microscopy (SEM) was done using FEGSEM, Thermo Scientific Quattro S. Energy dispersive spectrometer (EDS) measurements were carried out using LEO 1455 VP. Infrared (IR) spectra were recorded on the Alpha Bruker FTIR spectrophotometer (model no. 200695, Berlin, Germany). ^{1}H NMR spectra were recorded on a Bruker DPX (600 MHz, London, UK). Melting points were determined in open capillaries on an electrically heated metal block.

2.4. Catalytic Dehydrogenation of Benzylamine. In a typical experiment, in a 50 mL Schlenk flask, 10 mL of NaOH (1.0 M) was added to the solution of $NiSO_4{\cdot}6H_2O$ (0.052 g, 0.2 mM) in 5 mL of H_2O and then the commercial NaOCl (10 ml, 14 mM, 5.25%, 0.7 M) was added dropwise with stirring, and a fine black particle was formed. Benzylamine (1.1 g, 10 mM) was added to the reaction mixture with

stirring for two hours and then $NaHSO_3$ (10 mL, 10%) was added to quench the excess of NaOCl. The reaction mixture was extracted with CH_2Cl_2, and the extracts were dried over Na_2SO_4 anhydrous. The product was isolated and characterized by comparing its spectroscopic data with an authentic sample where appropriate [35] as follows:

Benzonitrile: b.p. 188–190°C; ^{1}H NMR (400 MHz, $CDCl_3$) δ: 7.44 (d, 2H, 2 × CH), 7.51 (d, 2H, 2 × CH), 7.54 (t, 1H, CH); IR (KBr, ν_{max}, cm^{-1}): 3067, 2229 cm^{-1} [35].

p-Methylbenzonitrile: m.p. 25–27°C; ^{1}H NMR (400 MHz, $CDCl_3$) δ: 7.23 (2H, d, J = 7.4 Hz, H-Ar), 7.47 (2H, d, J = 7.4 Hz, H-Ar). IR (KBr, ν_{max}, cm^{-1}): 3055, 2224 cm^{-1} [35].

p-Methoxybenzonitrile: m.p. 56–57°C; ^{1}H NMR (400 MHz, $CDCl_3$) δ: 3.881 (s, 3H CH_3O), 6.977 (d, 2H, ArH), 7.599 (d, 2H, ArH). IR (KBr, ν_{max}, cm^{-1}): 3060, 2232 cm^{-1} [35].

p-Hydroxybenzonitrile: m.p. 109–110°C; ^{1}H NMR (400 MHz, $CDCl_3$) δ: 6.014 (s, 1H, OH), 6.954 (d, 2H, ArH), 7.558 (d, 2H, ArH). IR (KBr, ν_{max}, cm^{-1}): 3062, 2229 cm^{-1} [35].

2.5. Recycling of Nickel Oxide. The produced NiO was washed by using acetone and water and then stirred with tenfold excess of NaOCl solution for 30 min. The recovered NiO_2 was used similarly as above (Section 3.2) for another dehydrogenation reaction.

3. Results and Discussion

3.1. Characterization of NiO_2 Nanoparticles

3.1.1. XRD Analysis. The X-ray diffraction pattern in Figure 1 displays the characteristic pattern of α-type NiO_2 nanoparticles formed with the assistance of NaOCl synthesis. The diffraction peaks observed at angles of 17.68°, 25.47°, 36.8°, and 61.48° corresponded to crystal planes (003), (006), (101), and (110), respectively. These peaks closely matched those found in JCPDS card no. 38-0715 [36]. The broadening of these peaks can be attributed to the formation of nanoparticles with a nanostructure, resulting in a smaller particle size [37]. Under the current experimental conditions, the broadening observed in certain diffraction peaks of NiO_2 nanoparticles XRD patterns could be attributed to the existence of minuscule particle-like structures. Furthermore, the XRD pattern exhibited "saw-tooth" reflections that are typical of two-dimensional turbostratic phases with layers that lack orientation [38]. The Debye–Scherer's equation was utilized to determine the average crystallite size of NPNP as follows [39]:

$$D = \frac{K\lambda}{\beta \cos\theta}, \tag{2}$$

where D is the average crystallite size, $\lambda = 1.54056$ Å is the wavelength of CuKα radiation, β is the full width at half-maximum (FWHM) intensity of the peak in radian, θ is Bragg's diffraction angle, and K is a constant usually equal to 0.9. Table 1 exposes that all XRD data of the sample and the estimated crystallite size (by using the Scherrer relation) found to vary between 11 nm and 29 nm (average 20 nm) for various identified diffraction peaks confirm the formation of the nanocrystalline structure which is in accordance with the TEM analyses.

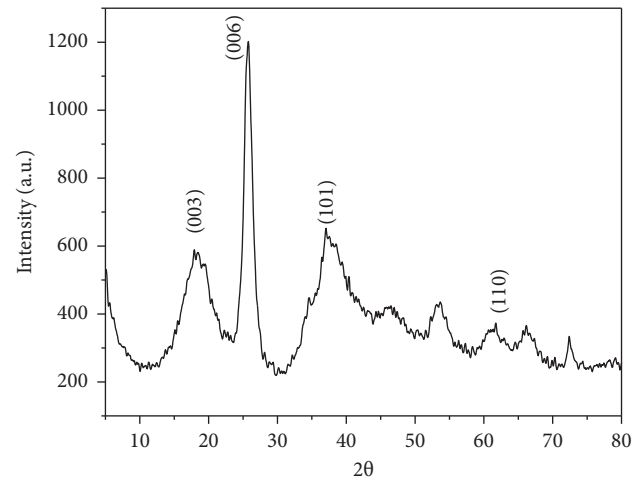

Figure 1: XRD diffractogram of the synthesized NiO_2.

3.1.2. SEM, TEM, and EDS. The SEM micrographs in Figure 2(a) exhibit the synthesized NiO_2 nanoparticles, indicating that the particles are spherical in shape and have formed nanoclusters due to the accumulation process. The nanosized crystallites may experience agglomeration because of their small size, which results in a large surface energy. This causes the nanocrystals to aggregate during crystal growth, thereby reducing their surface energy. The SEM images reveal that the average size of the observed NPNP is 24 nm. The evaluation of crystallinity was performed by comparing the crystallite size determined through SEM analysis. The resulting crystallinity index is presented in the following:

$$I = \frac{\mathrm{Dp\,(SEM)}}{\mathrm{Dcry\,(XRD)}}. \tag{3}$$

The crystallinity index, denoted as I_{cry}, was determined using the following parameters: $D_p = 24$ nm for the crystallite size (obtained from SEM image) and $D_{cry} = 20$ nm for the crystallite size (calculated from the Debye–Scherrer equation). Since the value of $I_{cry} = 1.2$ is higher than one, it is inferred that the crystallite size corresponds to a polycrystalline structure [40].

The transmission electron microscopy (TEM) analysis of the NiO_2 nanoparticles, as illustrated in Figure 2(b), revealed their uniform size characterized by spherical shapes and smooth surfaces, exhibiting even distribution. Nevertheless, the small size and high surface energy of

Table 1: XRD data of NPNP.

2θ	D value (Å)	Peak intensity (%)	Crystal planes	Crystallite size (nm)
17.68°	5.017	49	(003)	22
25.47°	3.496	100	(006)	11
36.82°	2.441	54	(101)	29
61.48°	1.508	31	(110)	18

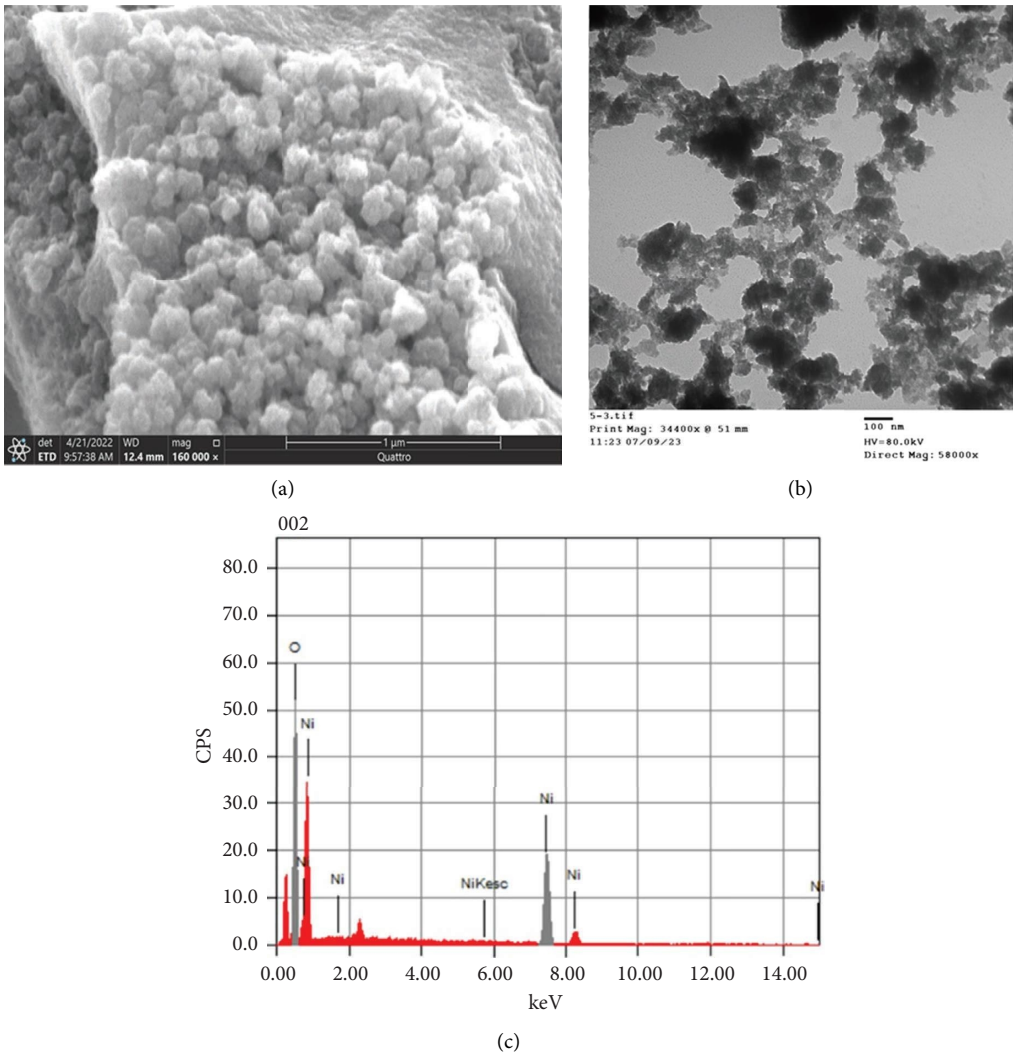

Figure 2: Morphology of NiO_2 catalyst: (a) SEM, (b) TEM, and (c) EDS.

some particles led to their aggregation into secondary particles [41]. In addition, the crystals consisted of mainly spherical particles with the size of 15–20 nm from the TEM observation, which is in good agreement with the result from the XRD patterns.

The EDS elemental analysis in Figure 2(c) confirms that the NiO_2 nanoparticles consist solely of Ni and O elements. However, the results obtained from EDS analysis (Table 2) reveal some deviations between theoretical and experimental values, which can be attributed to the presence of water attached to the NPNP [42].

3.1.3. FTIR Spectrum NiO_2 Nanoparticles. The FTIR spectrum of the NiO_2 nanoparticles sample exhibited typical features of NPNP. The observed spectrum exhibited a significant and wide peak at 3390 cm^{-1}, indicating the stretching vibration of O-H bonds in interlayer water molecules and hydrogen-bonded OH groups. However, the distinct peak associated with the stretching mode of independent Ni-OH groups was not present due to the hydrogen bonding occurring between hydrogen atoms and intercalated anions or water molecules within the layers. In addition, the peak at 1622 cm^{-1} was assigned to the bending

Table 2: The EDS data obtained from the elemental analysis of the NiO_2 nanoparticles.

Experimental			Calculated		
Ni	O	Ni/O	Ni	O	Ni/O
62.7	37.3	1.68	64.71	35.29	1.83

vibration of water. The bands due to carbonate ion are too weak to be identified, suggesting a low carbonate ion content. The band at 1370 cm^{-1} was characteristic of interlayer SO_4^{2-} stretching vibration resulted as a contaminant during the preparation process; the vibration at approximately 660 cm^{-1} was associated with Ni-O-H bonds, whereas a minor and faint vibration centered around 570 cm^{-1} was attributed to Ni-O stretching [43–45]. The FTIR spectrum of NiO_2 nanoparticles in Figure 3 displays significant absorption bands. The absorption band in the 500–700 cm^{-1} range indicates nanocrystals, and the small sample size caused the IR band associated with Ni-O stretching vibration to shift towards the blue region. This shift is due to quantum size effect and spherical nanostructures of NPNP [41].

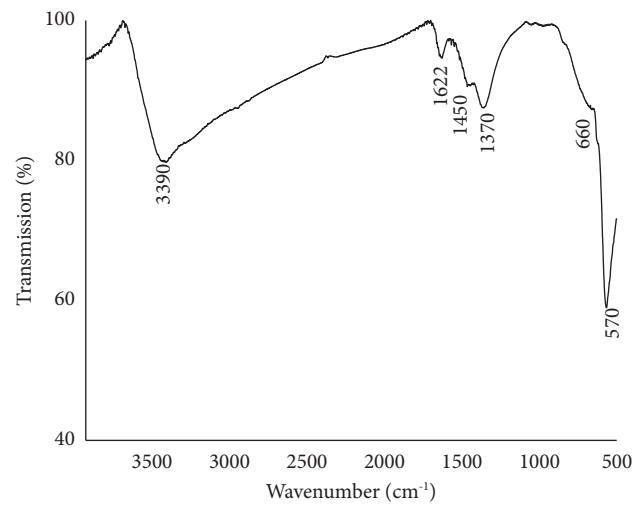

Figure 3: FTIR spectrum of NiO_2 nanoparticles.

3.2. Catalytic Dehydrogenation of Benzyl Amine. Yamazaki [46] reported the stoichiometric dehydrogenation of benzylamine to benzonitrile by NaOCl in ethanol; this encouraged us to investigate the catalytic dehydrogenation of benzylamine and some parasubstituents containing electron-donating and electron-withdrawing groups by the catalytic system $NiSO_4{\cdot}6H_2O$/NaOCl/NaOH (pH = 14) to their corresponding nitriles, as shown in Scheme 1.

Benzylamine was selected as a model substrate for the optimization of the reaction conditions. The results are given in Table 3.

Benzylamine was dehydrogenated by the in situ-generated NiO_2 nanoparticles to benzonitrile and water according to the following equation:

$$2NiO_2 + PhCH_2NH_2 \longrightarrow 2NiO + PhCN + 2H_2O \quad (4)$$

A set of experiments were carried out by the catalytic system $NiSO_4{\cdot}6H_2O$ (0.2 mM)/NaOCl (20 mL, 5.25%)/NaOH (10 mL, 1.0 M) (entry 1, Table 3).

It was found that benzylamine (10 mM) was smoothly dehydrogenated to benzonitrile in 95% yield within two hours.

On the other hand, a control experiment was performed in the absence of $NiSO_4{\cdot}6H_2O$; the yield of benzonitrile was 20% (entry 2, Table 3). This result is in agreement with the reported stoichiometric dehydrogenation of benzylamine [46].

The effect of the amount of $NiSO_4{\cdot}6H_2O$ on the yield of benzonotrile was studied by performing two reactions; it was found that the yield of benzonitrile was not improved. That is because the experiments with 0.1 mM and 0.3 mM of $NiSO_4{\cdot}6H_2O$ gave 51% and 94% of benzonitrile, respectively (entries 3 and 4, Table 3).

The effect of the amount of the co-oxidant was investigated by conducting one experiment with 5 mL of NaOCl (5.25%) and another one with 10 mL of NaOCl (5.25%). The yields of benzonitrile were 50% and 60%, respectively (entries 5 and 6, Table 3); these results were probably because the amount of the produced NiO_2 was not enough to dehydrogenate the whole amount of benzylamine and this consequently led to the formation of some other biproducts such as benzaldehyde and *N*-benzylidenebenzylamine.

To study the effect of the reaction time, two experiments were conducted under the same conditions of entry 1 but with different reaction times, 0.5 h and 1 h, and it was found that the yields of benzonitrile were 35% and 44%, respectively (entries 7 and 8, Table 3). These low yields were probably because these reaction times did not allow the catalytic dehydrogenation to go to completion in addition to the formation of some other side products like N-benzylidenebenzylamine.

3.2.1. The Produced NiO. The obtained NiO (equation (1)) powder was filtered and washed with deionized water and recycled by treatment with NaOCl and NaOH to produce NiO_2 nanoparticles that were used for the dehydrogenation of 10 mM of benzylamine. The yield obtained was 80% of benzonitrile (entries 9, Table 3); this recycling process was repeated two times and gave 60% and 55% of benzonitrile, respectively (entry 10 and 11, Table 3). The observed low yields in the recycling process can be attributed to the catalyst's loss during the reaction workup, as well as the loss of its active sites.

3.2.2. Reaction Conditions. All reactions were conducted at room temperature using 20 ml of NaOCl (5.25%), 10 mL of NaOH (1.0 M), 0.2 mM $NiSO_4{\cdot}6H_2O$, and 10 mM of benzylamine. Entries 2, 3, and 4 are as follows: the amounts of $NiSO_4{\cdot}6H_2O$ were 0.1, 0.3, and 0 mM, respectively. Entries 5 and 6 are as follows: the amounts of NaOCl (5%) were 5 mL and 10 mL, respectively. Entries 7 and 8 are as follows: the reaction times were 0.5 h and 1 h, respectively. Entries 9, 10, and 11 are the recycling of the produced NiO powder after

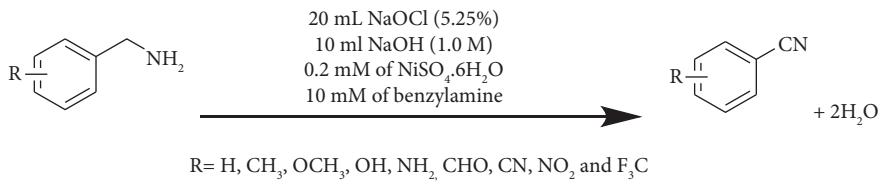

Scheme 1: Catalytic dehydrogenation of benzylamine and some p-substituted benzylamine by the catalytic system $NiSO_4{\cdot}6H_2O$/NaOCl/NaOH.

Table 3: Optimization of the reaction conditions for the catalytic dehydrogenation of benzylamine to benzonitrile by NPNP.

Entry	Y (%)	TO	TOF (h^{-1})
1	95	47.5	23.75
2	20	10	5
3	51	25.5	12.5
4	94	47	23.5
5	50	25	12.5
6	60	30	15
7	35	17.5	8.75
8	44	22	11
9	80	40	20
10	60	30	15
11	55	27.5	13.75

the workup. Y = yield (%) = number of moles of produced nitrile × 100/number of moles of benzylamine; TO = turn over = number of moles of product/number of moles of catalyst; TOF (h^{-1}) = turn over frequency = number of moles of product/number of moles of catalyst per hour.

The effect of the parasubstituents on the yield of the nitrile was studied via the dehydrogenation of four substituents containing electron-donating groups (p-CH_3, p-CH_3O, OH, and NH_2) and four substituents containing electron-withdrawing groups (p-CHO, p-CN, p-NO_2, and p-CF_3).

It was noticed that the yields that were found with the electron-withdrawing group (entries 16, 17, 18, and 19, Table 4) were lower than those with the electron-donating substituents (entries 12, 13, 14, and 15, Table 4).

The reason behind these observations could be attributed to the activation of the ring by electron-donating groups, which leads to an increase in the dehydrogenation of benzylamine into the corresponding nitrile. Conversely, electron-withdrawing groups deactivate the phenyl ring, causing a slowdown in the catalytic dehydrogenation process.

The reaction exhibited self-indication, as evidenced by the color change of the reaction mixture from green to black upon the addition of NaOCl, indicating the formation of NPNP. Over time, this color gradually disappeared with the formation of NiO. However, this catalytic dehydrogenation reaction is considered to be selective and catalytic (benzylamine is converted mainly to benzonitrile) and inexpensive. In addition, dehydrogenation was performed at room temperature. However, the obtained results were analogous with some recently reported protocols for the catalytic dehydrogenation of benzylamine but it is appeared to be superior, simpler, and more practical than the most previously reported approaches [47–49]. Dutta et al. reported the dehydrogenation of benzylamine to benzonitrile by a ruthenium(II) complex bearing a naphthyridine-functionalized pyrazole ligand in 84% yield in toluene and at 70°C [50] (our protocol did use any organic additive or organic solvent). Benzonitrile was obtained from benzylamine in 80% yield after 24 hours in dichloroethane as a solvent and at 110°C (higher temperature and longer reaction time than those applied in this catalytic system) [51]. Recently, the complex $[RuCl_2(p\text{-cymene})]_2$ catalyzed the conversion of benzylamine to nitrile in dichlorobenzene and in the presence of Me_4NCl at 150°C [52] (here, water was used as an ecofriendly solvent). Benzonitrile was produced from the photocatalytic oxidation of benzylamine by zirconium trisulfide (ZrS_3) but the workup is complicated and involved many steps [53]. To conclude, this protocol was highly selective, producing only nitrile as the product, and water as the sole byproduct. Moreover, it was free from the use of any toxic solvent or chemical.

3.3. Mechanism of Catalysis. The time-dependent profile illustrated the mechanism of dehydrogenation of benzylamine to benzonitrile through tracing the amount of benzylamine (% $BzNH_2$) and the produced amount of benzonitrile (% BzCN) with time. As expected, the amount of benzylamine was decreased and the amount of benzonitrile was increased, as shown in Figure 4.

The in situ-generated NiO_2 nanoparticles that were produced from the reaction of $NiSO_4{\cdot}6H_2O$ with NaOCl and in the presence of NaOH (equation (1)) were attacked by benzylamine forming the unstable intermediate $PhCH_2NH_2NiO_2$ (equation (5)), which is further dehydrogenated through the hydride abstraction mechanism [54]

Table 4: The scope of the catalytic dehydrogenation of benzylamines to nitriles NPNP.

Entries	Substrates	Products	Y (%)	TO	TOF (h^{-1})
12	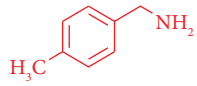	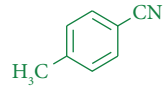	93	45.5	22.75
13	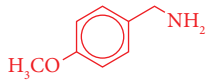	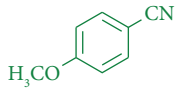	92	46	23
14	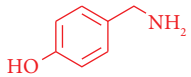	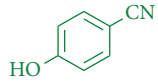	94	47	23.5
15	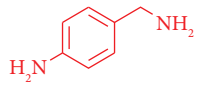	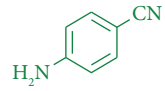	95	47.5	23.75
16	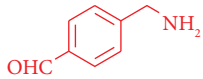	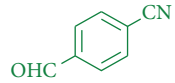	80	40	20
17	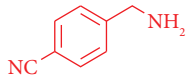	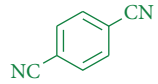	77	38.5	19.25
18	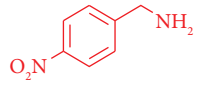	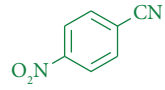	75	37.5	18.75
19	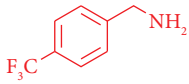	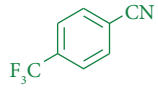	72	36	18

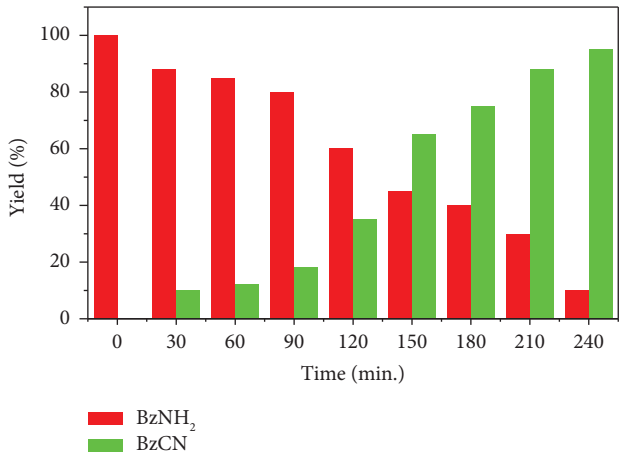

Figure 4: The time-dependent profile: the red column is the percentage yield of benzylamie ($BzNH_2$) and the green column is the percentage yield of benzonitrile (BzCN) with different time intervals.

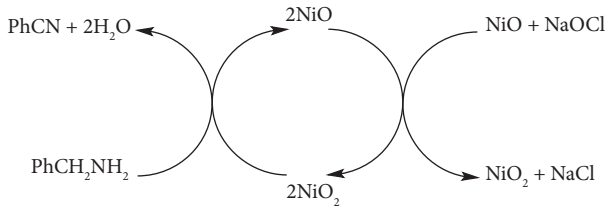

Scheme 2: Catalytic cycle of the dehydrogenation of benzylamine to benzonitrile by NPNP.

to liberate the corresponding imine (equation (6)). This imine reacted with one another molecule of NiO_2 to form the unstable $PhCHNHNiO_2$ (equation (7)) that underwent dehydrogenation to liberate benzonitrile and water (equation (8)).

$$NiO_2 + PhCH_2NH_2 \longrightarrow PhCH_2NH_2NiO_2 \quad (5)$$

$$PhCH_2NH_2NiO_2 \longrightarrow NiO + PhCHNH + H_2O \quad (6)$$

$$NiO_2 + PhCHNH \longrightarrow PhCHNHNiO_2 \quad (7)$$

$$PhCHNHNiO_2 \longrightarrow NiO + PhCN + H_2O \quad (8)$$

The produced NiO is further oxidized by the excess of NaOCl to produce NiO_2 as follows:

$$NiO + NaOCl \longrightarrow NiO_2 + NaCl \quad (9)$$

This catalytic cycle was repeated until the amount of benzylamine was completely consumed, as shown in Scheme 2.

4. Conclusion

$NiSO_4{\cdot}6H_2O$ and NaOCl in the presence of aqueous 1.0 molar KOH were used to generate NiO_2 nanoparticles. The particles were characterized and found to be spherical in shape with an average size of 20 nm, confirming their nanocrystalline structure. The catalytic system showed good performance in the dehydrogenation of benzylamine and some parasubstituents to benzonitriles. Optimum reaction conditions were determined, and the yields, turnover, and turnover frequency were calculated. The reaction mechanism was analyzed, and it was determined that the in situ-generated NPNP was the active species accountable for the dehydrogenation process. This promising reaction has several advantages as follows: the chemicals are inexpensive, water is used as a solvent at ambient temperature, the yields and turnover are good, and the produced NiO can be recycled for further catalytic reactions.

Data Availability

The datasets generated and analyzed during the current study are available from the corresponding author upon request.

Ethical Approval

All authors have read, understood, and have complied as applicable with the statement on "Ethical responsibilities."

Conflicts of Interest

The authors declare that they have no conflicts of interest.

Authors' Contributions

Shoair was the research director and performed objection discussion and article screening. Khalaf performed data interpretation, rote the characterization section and revised the final form. Almalki performed data extraction, methodology, and literature quality evaluation. Shanab and Nasef performed data extraction, methodology, and meta-analysis. Sheta performed study designing and article-draft writing. El-Basiony performed article-draft writing. Nasef performed data extraction, proposed the methodology, and performed meta-analysis. All the authors agreed with the final version of the article and the authors list. All the authors have read and approved the final manuscript.

Acknowledgments

The authors would like to thank the Deanship of Scientific Research, Taif University, Saudi Arabia, for supporting this work.

References

[1] P. T. Anastas and J. C. Warner, *Frontiers, Green Chemistry: Theory and Practice*, Oxford University Press, Oxford, UK, vol. 640, p. 1998, 1998.

[2] F. F. Fleming, L. Yao, P. Ravikumar, L. Funk, and B. C. Shook, "Nitrile-containing pharmaceuticals: efficacious roles of the nitrile pharmacophore," *Journal of Medicinal Chemistry*, vol. 53, no. 22, pp. 7902–7917, 2010.

[3] L. M. Dornan, Q. Cao, and M. J. Muldoon, "Green oxidative synthesis of nitriles," in *Green Oxidation in Organic Synthesis*, pp. 199–220, Springer, Berlin, Germany, 2019.

[4] X. Wang, Y. Wang, X. Li, Z. Yu, C. Song, and Y. Du, "Nitrile-containing pharmaceuticals: target, mechanism of action, and their SAR studies," *RSC Medicinal Chemistry*, vol. 12, no. 10, pp. 1650–1671, 2021.

[5] C. Galli, "Radical reactions of arenediazonium ions: an easy entry into the chemistry of the aryl radical," *Chemical Reviews*, vol. 88, no. 5, pp. 765–792, 1988.

[6] H.-J. Cristau, A. Ouali, J.-F. Spindler, and M. Taillefer, "Mild and efficient copper-catalyzed cyanation of aryl iodides and bromides," *Chemistry-A European Journal*, vol. 11, no. 8, pp. 2483–2492, 2005.

[7] Z. Chen, W. Chen, L. Zhang et al., "Acidic hierarchical porous ZSM-5 assembled palladium catalyst: a green substitute to transform primary amides to nitriles," *Applied Catalysis B: Environmental*, vol. 302, Article ID 120835, 2022.

[8] F. G. Buono, R. Chidambaram, R. H. Mueller, and R. E. Waltermire, "Insights into palladium-catalyzed cyanation of bromobenzene: additive effects on the rate-limiting step," *Organic Letters*, vol. 10, no. 23, pp. 5325–5328, 2008.

[9] R. Ray, A. S. Hazari, G. K. Lahiri, and D. Maiti, "Ruthenium-catalyzed aerobic oxidation of amines," *Chemistry--An Asian Journal*, vol. 13, no. 17, pp. 2138–2148, 2018.

[10] W. P. Griffith, B. Reddy, A. G. Shoair, M. Suriaatmaja, A. J. White, and D. J. Williams, "Ruthenate(VI)-catalysed dehydrogenation of primary amines to nitriles, and crystal structures of cis-[Ru(bipy)2(NH2CH2Ph)2] [PF6]2·0.5MeOH and cis-[Ru(bipy)2(NCPh)2] [PF6]2·CH2Cl2," *Journal of the Chemical Society, Dalton Transactions*, no. 17, pp. 2819–2826, 1998.

[11] S. E. Diamond, G. M. Tom, and H. Taube, "Ruthenium promoted oxidation of amines," *Journal of the American Chemical Society*, vol. 97, no. 10, pp. 2661–2664, 1975.

[12] B. Xu, E. M. Hartigan, G. Feula, Z. Huang, J. P. Lumb, and B. A. Arndtsen, "Simple copper catalysts for the aerobic

oxidation of amines: selectivity control by the counterion," *Angewandte Chemie*, vol. 128, no. 51, pp. 16034–16038, 2016.

[13] Y. Maeda, T. Nishimura, and S. Uemura, "Copper-catalyzed oxidation of amines with molecular oxygen," *Bulletin of the Chemical Society of Japan*, vol. 76, no. 12, pp. 2399–2403, 2003.

[14] M. George and K. Balachandran, "Nickel-peroxide oxidation of organic compounds," *Chemical Reviews*, vol. 75, no. 4, pp. 491–519, 1975.

[15] K. Nakagawa and T. Tsuji, "Oxidation with nickel peroxide. II. Oxidation of amines," *Chemical and Pharmaceutical Bulletin*, vol. 11, no. 3, pp. 296–301, 1963.

[16] Z. Fang, Y. Ding, M. Wang et al., "Synthesis of nitriles by the electro-oxidative coupling of primary alcohols and ammonia on Pd nanoparticle-modified CuO nanowires in oxidant-free electrolytes under ambient conditions," *Applied Catalysis B: Environmental*, vol. 337, Article ID 122999, 2023.

[17] Q. Xiao, Y. Feng, L. Chen et al., "Engineered aldoxime dehydratase to enable the chemoenzymatic conversion of benzyl amines to aromatic nitriles," *Bioorganic Chemistry*, vol. 134, Article ID 106468, 2023.

[18] S. Kumar, A. Jain, S. Panwar et al., "Antibacterial studies of ZnO and silica capped manganese doped zinc sulphide nanostructures," *Applied Physics A*, vol. 129, no. 3, p. 169, 2023.

[19] S. Kumar, H. Bhatti, H. S. Bhatti et al., "Effect of glutathione capping on the antibacterial activity of tin doped ZnO nanoparticles," *Physica Scripta*, vol. 96, no. 12, Article ID 125807, 2021.

[20] V. K. Magotra, T. Kang, A. T. Aqueel Ahmed et al., "Effect of gold nanoparticles laced anode on the bio-electro-catalytic activity and power generation ability of compost based microbial fuel cell as a coin cell sized device," *Biomass and Bioenergy*, vol. 152, Article ID 106200, 2021.

[21] S. Kumar, S. Taneja, S. Banyal et al., "Bio-synthesised silver nanoparticle-conjugated l-cysteine ceiled Mn:ZnS quantum dots for eco-friendly biosensor and antimicrobial applications," *Journal of Electronic Materials*, vol. 50, no. 7, pp. 3986–3995, 2021.

[22] H. A.-F. Khalaf and R. F. A. El-Baki, "Effectiveness of ceria and stania nanoparticles in photodegradation tenoxicam antibiotics using UV-H2O2," *Iranian Journal of Catalysis*, vol. 13, no. 3, pp. 285–297, 2023.

[23] S. Tomar, S. Gupta, A. Priyam et al., "Temporal evolution of optical absorption and emission spectra of thiol capped CdTe quantum dots," *Applied Physics A*, vol. 128, no. 10, p. 944, 2022.

[24] A. Navinprasad, R. Prakash, J. Yoganandh, B. Meenakshipriya, and K. Ramakrishnan, "Experimental investigation of nickel oxide nanomaterials with n-pentane diesel blends in compression ignition engine," in *IOP Conference Series: Materials Science and Engineering*, IOP Publishing, Bristol, UK, 2021.

[25] U. Shuaib, T. Hussain, R. Ahmad et al., "Novel synthesis of nickel oxide-copper hexacyanoferrate binary hybrid nanocomposite for high-performance supercapacitor application," *Journal of Solid State Electrochemistry*, vol. 27, no. 3, pp. 715–725, 2023.

[26] V. Kumar, D. Raj, S. K. Chakarvarti, R. K. Choubey, and S. Kumar, "Solvothermal growth of ultrathin nonporous nickel oxide nanosheets for ethanol sensing," *Journal of Materials Science: Materials in Electronics*, vol. 32, no. 1, pp. 818–826, 2021.

[27] D. Lee and M. Van Den Engh, *WS Trahanovsky*, Academic Press, New York, NY, USA, 1973.

[28] J. Skarzewski and R. Siedlecka, "Organic preparations and procedures international," *The New Journal for Organic Synthesis*, vol. 24, no. 6, pp. 623–647, 1992.

[29] A. S. Almalki, "Synthesis and characterization of 3-(aryl azo)-4-hydroxy-1,2-naphthoquinone ruthenium(III) complexes as catalysts for benzyl alcohol oxidation," *Chemistry Select*, vol. 6, no. 29, pp. 7525–7536, 2021.

[30] A. G. F. Shoair, M. M. Shanab, and M. H. Mahmoud, "Electrochemical and catalytic properties of oxo-ruthenate(VI) in aqueous alkaline medium," *International Journal of Electrochemical Science*, vol. 16, no. 5, Article ID 210545, 2021.

[31] A. G. F. Shoair, M. M. Shanab, N. A. El-Ghamaz, M. M. Abou-Krisha, S. H. Kenawy, and T. A. Yousef, "Green catalytic conversion of some benzylic alcohols to acids by NiO2 nanoparticles (NPNPs) in water," *Catalysts*, vol. 13, no. 4, p. 645, 2023.

[32] H. Ji, T. Wang, M. Zhang, Y. She, and L. Wang, "Simple fabrication of nano-sized NiO2 powder and its application to oxidation reactions," *Applied Catalysis A: General*, vol. 282, no. 1-2, pp. 25–30, 2005.

[33] S. Kinra, M. P. Ghosh, S. Mohanty, R. K. Choubey, and S. Mukherjee, "Manganese ions substituted ZnO nanoparticles: synthesis, microstructural and optical properties," *Physica B: Condensed Matter*, vol. 627, Article ID 413523, 2022.

[34] S. Kinra, M. P. Ghosh, S. Mohanty, R. K. Choubey, and S. Mukherjee, "Correlating the microstructural and optical properties of vanadium ion-doped ZnO nanocrystals," *Bulletin of Materials Science*, vol. 45, no. 2, p. 65, 2022.

[35] S. K. Dewan, R. Singh, and A. Kumar, "One pot synthesis of nitriles from aldehydes and hydroxylamine hydrochloride using sodium sulphate (anhyd) and sodium bicarbonate in dry media under microwave irradiation," *Arkivoc*, vol. 2, pp. 41–44, 2006.

[36] D. Mohammadyani, S. Hosseini, and S. Sadrnezhaad, "Characterization of nickel oxide nanoparticles synthesized via rapid microwave-assisted route," in *International Journal of Modern Physics: Conference Series*, World Scientific, Singapore, 2012.

[37] E. Bulut and M. Ozacar, "Rapid, facile synthesis of silver nanostructure using hydrolyzable tannin," *Industrial and Engineering Chemistry Research*, vol. 48, no. 12, pp. 5686–5690, 2009.

[38] G.-R. Fu, Z.-A. Hu, L.-J. Xie et al., "Electrodeposition of nickel hydroxide films on nickel foil and its electrochemical performances for supercapacitor," *International Journal of Electrochemical Science*, vol. 4, no. 8, pp. 1052–1062, 2009.

[39] B. D. Cullity, *Elements of X-ray Diffraction*, Addison-Wesley Publishing, Boston, MA, USA, 1956.

[40] A. Rahdar, M. Aliahmad, and Y. Azizi, "NiO nanoparticles: synthesis and characterization," *Journal of Nanostructures*, vol. 5, pp. 145–151, 2015.

[41] H. Qiao, Z. Wei, H. Yang, L. Zhu, and X. Yan, "Preparation and characterization of NiO nanoparticles by anodic arc plasma method," *Journal of Nanomaterials*, vol. 2009, Article ID 795928, 5 pages, 2009.

[42] M. Kooti and M. Jorfi, "Synthesis and characterization of nanosized NiO2 and NiO using Triton® X-100," *Open Chemistry*, vol. 7, no. 1, pp. 155–158, 2009.

[43] L.-X. Yang, Y.-J. Zhu, H. Tong, Z.-H. Liang, L. Li, and L. Zhang, "Hydrothermal synthesis of nickel hydroxide nanostructures in mixed solvents of water and alcohol,"

Journal of Solid State Chemistry, vol. 180, no. 7, pp. 2095–2101, 2007.

[44] Z. Cheng, J. Xu, H. Zhong, D. Li, P. Zhu, and Y. Yang, "A facile and novel synthetic route to nanoflowers," *Superlattices and Microstructures*, vol. 48, no. 2, pp. 154–161, 2010.

[45] U. Shuaib, D. Lee, T. Hussain et al., "Green synthesis of nickel oxide coupled copper hexacyanoferrate (NiO2–CuHCF) nanocomposites for efficient and highly stable natural sunlight-driven photocatalytic degradation of wastewater pollutants," *Ceramics International*, vol. 48, no. 18, pp. 26168–26176, 2022.

[46] S. Yamazaki, "A simple and convenient method for the synthesis of nitriles by oxidation of primary amines with NaOCl in ethanol," *Synthetic Communications*, vol. 27, no. 20, pp. 3559–3564, 1997.

[47] T. Ali, H. Wang, W. Iqbal, T. Bashir, R. Shah, and Y. Hu, "Electro-synthesis of organic compounds with heterogeneous catalysis," *Advanced Science*, vol. 10, no. 1, Article ID 2205077, 2022.

[48] M. T. Bender and K.-S. Choi, "Electrochemical dehydrogenation pathways of amines to nitriles on NiOOH," *Journal of the American Chemical Society (JACS)*, vol. 2, no. 5, pp. 1169–1180, 2022.

[49] S. Bai, L. Chen, J. Bai et al., "V modified Ni-based layer hydroxides for the electrocatalytic upgrading of amines to nitriles," *Inorganic Chemistry Frontiers*, vol. 10, no. 16, pp. 4695–4701, 2023.

[50] I. Dutta, S. Yadav, A. Sarbajna et al., "Double dehydrogenation of primary amines to nitriles by a ruthenium complex featuring pyrazole functionality," *Journal of the American Chemical Society*, vol. 140, no. 28, pp. 8662–8666, 2018.

[51] T. Achard, J. Egly, M. Sigrist, A. Maisse-François, and S. Bellemin-Laponnaz, "Easy ruthenium-catalysed oxidation of primary amines to nitriles under oxidant-free conditions," *Chemistry--A European Journal*, vol. 25, no. 58, pp. 13271–13274, 2019.

[52] M. Olivares, P. Knörr, and M. Albrecht, "Aerobic dehydrogenation of amines to nitriles catalyzed by triazolylidene ruthenium complexes with O_2 as terminal oxidant," *Dalton Transactions*, vol. 49, no. 6, pp. 1981–1991, 2020.

[53] Z. Tian, C. Han, Y. Zhao et al., "Efficient photocatalytic hydrogen peroxide generation coupled with selective benzylamine oxidation over defective ZrS3 nanobelts," *Nature Communications*, vol. 12, no. 1, p. 2039, 2021.

[54] J. L. Miller, J.-M. I. Lawrence, F. O. R. Del Rey, and P. E. Floreancig, "Synthetic applications of hydride abstraction reactions by organic oxidants," *Chemical Society Reviews*, vol. 51, no. 13, pp. 5660–5690, 2022.